

Prediction of Survival After Pediatric Cardiac Arrest Using Quantitative EEG and Machine Learning Techniques

Hunfeld, Maayke; Verboom, Marit; Josemans, Sabine; van Ravensberg, Annemiek; Straver, Dirk; Lückérath, Femke; Jongbloed, Geurt; Buysse, Corinne; van den Berg, Robert

DOI

[10.1212/WNL.0000000000210043](https://doi.org/10.1212/WNL.0000000000210043)

Publication date

2024

Document Version

Final published version

Published in

Neurology

Citation (APA)

Hunfeld, M., Verboom, M., Josemans, S., van Ravensberg, A., Straver, D., Lückérath, F., Jongbloed, G., Buysse, C., & van den Berg, R. (2024). Prediction of Survival After Pediatric Cardiac Arrest Using Quantitative EEG and Machine Learning Techniques. *Neurology*, *103*(12), Article e210043. <https://doi.org/10.1212/WNL.0000000000210043>

Important note

To cite this publication, please use the final published version (if applicable). Please check the document version above.

Copyright

Other than for strictly personal use, it is not permitted to download, forward or distribute the text or part of it, without the consent of the author(s) and/or copyright holder(s), unless the work is under an open content license such as Creative Commons.

Takedown policy

Please contact us and provide details if you believe this document breaches copyrights. We will remove access to the work immediately and investigate your claim.

Green Open Access added to TU Delft Institutional Repository

'You share, we take care!' - Taverne project

<https://www.openaccess.nl/en/you-share-we-take-care>

Otherwise as indicated in the copyright section: the publisher is the copyright holder of this work and the author uses the Dutch legislation to make this work public.

Prediction of Survival After Pediatric Cardiac Arrest Using Quantitative EEG and Machine Learning Techniques

Maayke Hunfeld, MD, PhD, Marit Verboom, MSc,* Sabine Josemans, MSc,* Annemiek van Ravensberg, MSc,* Dirk Straver, MD, PhD, Femke Lückérath, MSc, Geurt Jongbloed, PhD, Corinne Buysse, MD, PhD, and Robert van den Berg, MD, PhD

Neurology® 2024;103:e210043. doi:10.1212/WNL.0000000000210043

Correspondence

Dr. van den Berg
r.vandenberg@
erasmusmc.nl

Abstract

Background and Objectives

Early neuroprognostication in children with reduced consciousness after cardiac arrest (CA) is a major clinical challenge. EEG is frequently used for neuroprognostication in adults, but has not been sufficiently validated for this indication in children. Using machine learning techniques, we studied the predictive value of quantitative EEG (qEEG) features for survival 12 months after CA, based on EEG recordings obtained 24 hours after CA in children. The results were confirmed through visual analysis of EEG background patterns.

Methods

This is a retrospective single-center study including children (0–17 years) with CA, who were subsequently admitted to the pediatric intensive care unit (PICU) of a tertiary care hospital between 2012 and 2021 after return of circulation (ROC) and were monitored using EEG at 24 hours after ROC. Signal features were extracted from a 30-minute EEG segment 24 hours after CA and used to train a random forest model. The background pattern from the same EEG fragment was visually classified. The primary outcome was survival or death 12 months after CA. Analysis of the prognostic accuracy of the model included calculation of receiver-operating characteristic and predictive values. Feature contribution to the model was analyzed using Shapley values.

Results

Eighty-six children were included (in-hospital CA 27%, out-of-hospital CA 73%). The median age at CA was 2.6 years; 53 (62%) were male. Mortality at 12 months was 56%; main causes of death on the PICU were withdrawal of life-sustaining therapies because of poor neurologic prognosis (52%) and brain death (31%). The random forest model was able to predict death at 12 months with an accuracy of 0.77 and positive predictive value of 1.0. Continuity and amplitude of the EEG signal were the signal parameters most contributing to the model classification. Visual analysis showed that no patients with a background pattern other than continuous with amplitudes exceeding 20 μ V were alive after 12 months.

Discussion

Both qEEG and visual EEG background classification for registrations obtained 24 hours after ROC form a strong predictor of nonsurvival 12 months after CA in children.

RELATED ARTICLE

Editorial

Advancing Pediatric Post-Arrest Care Using Quantitative EEG

Page e210147

*These authors contributed equally to this work.

From the Department of Neurology (M.H., M.V., S.J., A.v.R., D.S., R.v.d.B.), Erasmus MC, University Medical Center; Department of Neonatal and Pediatric Intensive Care, Division of Pediatric Intensive Care (M.H., C.B.), Erasmus MC Children's Hospital, Rotterdam; and Delft Institute of Applied Mathematics (F.L., G.J.), Delft University of Technology, the Netherlands.

Go to [Neurology.org/N](https://www.neurology.org/N) for full disclosures. Funding information and disclosures deemed relevant by the authors, if any, are provided at the end of the article.

Glossary

ACNS = American Clinical Neurophysiology Society; AUC = area under the curve; CA = cardiac arrest; cEEG = continuous EEG; ESR = EEG silence ratio; GPD = generalized periodic discharge; IHCA = in-hospital cardiac arrest; ML = machine learning; OHCA = out-of-hospital cardiac arrest; PCPC = pediatric cerebral performance category; PICU = pediatric intensive care unit; qEEG = quantitative EEG; ROC = return of circulation; SHAP = Shapley Additive Explanations.

Introduction

Each year 15,000 children experience an in-hospital cardiac arrest (IHCA) and approximately 6,000 an out-of-hospital cardiac arrest (OHCA) in the United States.¹⁻³ Mortality is still high; approximately 89% of children with OHCA and 58% of children with IHCA die before hospital discharge.⁴⁻⁷ Predicting precise long-term outcomes in children who have reached return of circulation (ROC) is a great challenge, particularly in those who remain unconscious after 24 hours. This is compounded by a lack of standardization for pediatric neuroprognostication in postanoxic coma.^{8,9} It is crucial to predict neurologic outcome as accurately as possible in these children to discuss further steps of treatment and to inform parents correctly. An inaccurate prediction of long-term outcome could lead to premature withdrawal of life-sustaining treatment or, at the other end of the spectrum, severely disabled children with persistent vegetative state, with a high impact on caregivers and resources.¹⁰

The EEG is frequently used for neuroprognostication, demonstrating significant sensitivity and specificity in predicting neurologic outcomes in adults with postanoxic encephalopathy.^{11,12} However, the application of EEG in pediatric neuroprognostication faces unique challenges, particularly the lack of adequately validated prognostic patterns for children.⁸ While some studies have identified EEG background patterns associated with neurologic outcomes at hospital discharge after cardiac arrest (CA), these lack standardized description, limiting their clinical utility.¹³⁻¹⁶ All EEG recordings in these studies were visually assessed, which is time-consuming and requires the expertise of an experienced electroencephalographer. Moreover, high inter-rater variability has been reported for visual EEG interpretation.¹⁷ Visual analysis of EEG inherently overlooks critical signal characteristics such as complexity and functional connectivity, which require mathematical preprocessing to assess. This limitation excludes potentially valuable information that cannot be detected through visual inspection alone.

To overcome the limitations of traditional visual EEG analysis, we explored the use of quantitative EEG (qEEG) combined with machine learning (ML) techniques. qEEG provides a mathematical and objective assessment of EEG signals, offering detailed insights that visual analysis misses. Training ML algorithms on qEEG features is an effective technique to predict the outcome in postanoxic encephalopathy in adults.¹⁸⁻²⁰ In contrast to the extensive literature on

prognostication in adults, only 1 study used qEEG in a similar role after pediatric CA,²¹ which used a limited set of qEEG features without comparing its prognostic accuracy with visual EEG assessment while a recent study evaluated the use of a single qEEG feature (suppression ratio) for prediction of cerebral injury.²² This highlights a significant research gap and underscores the need for comprehensive studies that evaluate the full potential of qEEG and ML in pediatric neuroprognostication.

We hypothesized that a more comprehensive set of qEEG features—encompassing time, frequency, connectivity, and entropy domains—will more accurately capture the complex dynamics of EEG signals. Such a set, analyzed through ML, can improve the prediction of outcomes of children after CA. Accordingly, the primary objective of this study was to identify EEG background patterns at 24 hours after ROC that correlate with survival 12 months after arrest. To achieve this, we adopted a dual approach: integrating the identification of relevant qEEG features by ML with parallel visual EEG analysis. This methodology aims to combine the objective precision of qEEG with the more nuanced insights provided by expert visual analysis, offering a comprehensive understanding of EEG's predictive value for post-CA outcomes in children.

Methods

Standard Protocol Approvals, Registrations, and Patient Consents

This retrospective study was performed at the pediatric intensive care unit (PICU) and clinical neurophysiology department of the Erasmus MC Sophia Children's Hospital in Rotterdam, a tertiary care university hospital, which provides health care to children in the southwest part of the Netherlands (referral area 4 million inhabitants, approximately 25% of the Dutch population). The Erasmus MC Ethical Review Board approved the study protocol (MEC-2019-0259 and MEC-2021-0145). The need to obtain informed consent was waived.

Patients

All children aged 0–17 years with IHCA or OHCA between 2012 and 2021 who were subsequently admitted to our PICU after ROC and were monitored using EEG 24 hours after ROC were eligible for inclusion. CA was defined as unresponsiveness with absent palpable pulse for at least 1 minute. Children with preexisting severe neurologic deficits

(defined as a prearrest Pediatric Cerebral Performance Category [PCPC]²³ score of >3, retrospectively derived by chart review [M.H.]); traumatic OHCA; or intracranial lesions such as intracranial hemorrhage, brain tumor, or meningitis as a cause of arrest were excluded.

Outcomes

The PCPC score determined 12 months after CA and dichotomized to survival (PCPC 1–5) and death (PCPC 6) was our primary measure of neurologic outcome. The decision to dichotomize was made before study initiation, based on findings of our previous work⁶; most of the children either survived with a good neurologic outcome or died before discharge. In our center, pediatric CA survivors are included in our multidisciplinary outpatient follow-up program (standard of care) with scheduled standardized visits (including at 12 months after CA) until the age of 18 years. The PCPC score was determined during a visit to this outpatient clinic, staffed by an experienced pediatric intensivist (C.B.) and pediatric neurologist (M.H.). When no follow-up visit took place, these outcomes were collected from notes in the patient records (e.g., based on hospital visits with other physicians).

EEG Registration

Between 2012 and 2016, EEGs after CA were performed based on clinical need as determined by the treating physicians. Recognizing the importance of systematic monitoring, since 2017, local guidelines recommend continuous EEG (cEEG) in all children with impaired consciousness after CA. All EEG recordings were analyzed retrospectively. EEG was recorded with an OSG BrainRT system (Rumst, Belgium) adhering to the International 10-20 System for electrode placement, with 11–19 electrodes depending on head circumference and a sampling rate of 256 Hz. Data were exported from BrainRT software in EDF+ format²⁴ for further analysis in a data structure that adheres to the EEG-BIDS specifications.²⁵

Quantified EEG Analysis

For qEEG analysis, we selected a 30-minute data segment at 24 hours after CA (from –15 to +15 minutes). This time frame was considered optimal for assessing brain function using EEG, based on findings in adult post-CA studies.²⁶ All patients were sedated at this time point. The raw data were filtered using a noncausal finite impulse response bandpass filter with a lower and upper passband edge at 0.5 and 35 Hz, respectively. A notch filter at 50 Hz was used to remove the remaining line noise. Epochs were visually inspected to identify and remove major artifacts and bad channels. Independent component analysis was used to identify and remove ECG artifacts. The resulting artifact-free epochs were re-referenced to a common average reference and split into subepochs with a duration of 20 seconds and overlap of 10 seconds, yielding an average of 158 epochs per patient (range 38–179). All preprocessing was performed using the MNE library in Python.²⁷

A set of 27 qEEG features was selected based on the results of previous studies in adults^{20,28,29} (Table 1), considering their power to describe a time signal in the time, frequency, connectivity, and entropy domains. These features were first calculated per epoch for each individual channel, and channel values were then averaged to generate a single value per feature per epoch. The feature calculations were performed in MATLAB version R2022a.³⁰

Random Forest Classifier

The calculated EEG features per epoch were used as input for a random forest classifier, with the primary clinical outcome (PCPC 12 months after diagnosis, dichotomized to survival/death) as the output label. In summary, the data set was split into test and training samples using a stratified K-fold cross-validator (Python Scikit-learn³¹) with a 5-fold split and a train/test ratio of 80/20. Stratification was used to preserve the ratio between outcome classes in the test and training subsets, with epochs from each patient exclusively allocated to either the test or training set to prevent data leakage. A grid search algorithm was used to find the optimal parameters for the random forest model. The model returns for each epoch a probability estimate between 0 and 1 for unfavorable outcome. To reduce the number of false positives, a probability of 0.7 was used as a threshold to label an epoch as unfavorable. Performance of the model was assessed with receiver operator characteristics analyses, including area under the curve (AUC), recall, and precision. A patient was predicted to have an unfavorable outcome if over 99% of all epochs for that patient were classified as unfavorable (eFigure 1). Enhancing our model's interpretability and evaluating the contribution of different EEG features to prognostic classification, we performed a Shapley Additive Explanations analysis (SHAP, Python Shap³²). This approach allowed us to assign a score to the contribution of each feature to the classification per epoch, strongly increasing the explainability of the model.

Visual EEG Analysis

To complement the quantitative analysis, the same 30-minute epochs were used for visual assessment. Two experienced clinical neurophysiologists (D.S., R.v.d.B.) who were blinded to the clinical outcome, independently reviewed each segment. They classified the EEG background patterns according to the American Clinical Neurophysiology Society (ACNS) Critical Care EEG terminology³³ and the Dutch national protocol for the prognosis of postanoxic encephalopathy in adults. In case of disagreement, both neurophysiologists convened to reach consensus. Interobserver agreement was analyzed using Cohen κ . The EEG backgrounds were categorized into 8 distinct patterns: (1) unusable due to artifacts, (2) continuous background pattern with amplitudes exceeding 20 μ V, (3) continuous background but with suppressed amplitudes (<20 μ V), (4) burst-suppression pattern with nonidentical bursts, (5) burst-suppression pattern with the first 500 milliseconds of each burst visually identical, (6) generalized periodic

Table 1 Description of Calculated EEG Features Included for Training the Random Forest Classifier

EEG feature	Feature description	Ref.
Amplitude features quantify the various aspects of the EEG signal's amplitude, which reflects the strength and variability of brain activity		
Amplitude descriptive statistics	The minimal, maximal, average, and range of amplitude per epoch in microvolts, calculated on the absolute values of the signal after applying a sliding window moving average with a window length of one-fourth of the sample rate of the signal	³⁰
Line length	Line length is defined as the running sum of the absolute differences between all consecutive samples within a predefined window	⁴⁵
Regularity	Regularity of the amplitude of a signal. A signal with low amplitude and short period of higher amplitudes (suppression, burst) has a value close to zero. Signals with higher continuous amplitudes have a higher regularity value	¹⁸
Complexity features are a measure of the regularity and unpredictability of EEG data. Lower values of these features indicate a more predictable and regular signal (e.g., an isoelectric or diffusely slow pattern) while higher values suggest greater complexity and irregularity (e.g., a continuous EEG pattern with varying frequencies)		
Approximate entropy	The approximate entropy calculates the predictability of future amplitude values in the EEG by considering the preceding amplitude values	³⁰
Sample entropy	Quantification of the uncertainty of stochastic signals in the frequency domain	⁴⁶
Tsallis entropy	Quantification of the uncertainty of stochastic signals in the frequency domain. It captures the complexity and regularity of a signal by analyzing the different frequency components of the signal	⁴⁷
Connectivity features provide insight into the functional organization of brain networks, for example, how different brain regions communicate. A high connectivity is characterized by synchronized, phase-consistent EEG signals between brain regions (electrodes) while more independent signals have low connectivity		
Phase-lag index	Measure for the asymmetry of the distribution of phase differences between signals recorded from different brain regions. A PLI value close to 0 suggests weak or no functional connectivity while a value close to 1 indicates strong phase consistency and stronger functional connectivity	⁴⁸
Coherence	Measure of the similarity between the PSD of 2 signals, indicating the degree of synchrony. Calculated separately for alpha, beta, theta, and delta band frequency components	³⁰
Continuity features describe how continuous the EEG signal is and range from 0 to 1. High values for BSR and/or ESR indicate that a large proportion of the EEG signal is suppressed or flat while a low value indicates a continuous signal. A feature value around 0.5 indicates a burst-suppression pattern		
BSR	The fraction of time in which the amplitude of the EEG signal is <5 μ V	
ESR	Intervals of suppression of >240 milliseconds during which the EEG signal is <5 μ V	⁴⁹
Frequency features in EEG analysis measure the power and distribution of brain activity across different frequency bands		
Absolute power	The average spectral power in frequency components of the signal based on a periodogram, calculated separately for alpha, beta, theta and delta band frequency ranges	³⁰
Relative power	The relative spectral power in the alpha, beta, and theta frequency bands relative to the spectral power in the delta frequency band	
SEF90	The frequency below which 90% of the total power of the signal is contained	
Hjorth features provide a concise characterization of EEG signals, describing overall power, signal regularity, and frequency variations		
Hjorth activity	The variance of a time signal. Activity increases for a signal with higher frequencies	⁵⁰
Hjorth complexity	The change in frequency and similarity to a sine wave. Hjorth complexity compares the similarity of the signal with a sine wave (a value of 1 means that the signal is more similar to a sine wave)	
Hjorth mobility	Hjorth mobility is a measure of the SD of the power spectrum	

Abbreviations: BSR = burst-suppression ratio; ESR = EEG silence ratio; PLI = phase-lag index; PSD = power spectral density; SEF = spectral edge frequency. In all cases where features are calculated for separate spectral frequency bands, these are defined as delta (0.5–4 Hz), theta (4–8 Hz), alpha (8–12 Hz), and beta (12–30 Hz).

discharges (GPDs) intermixed with other activity (nonflat background), (7) GPDs on a background with no other cerebral activity, and (8) isoelectric background with no discernible cerebral activity. To gain more insight into the classification of the random forest model, the categorization of the background pattern as other than continuous with

amplitudes exceeding 20 μ V was compared with prediction of unfavorable outcome by the model.

Data Availability

Anonymized data and code will be made available upon request from qualified investigators.

Results

Patient Sample

Of a total of 459 children in our data set with CA between 2012 and 2021 (IHCA n = 246 [54%] and OHCA n = 213 [45%]), 393 achieved ROC (86%), of which 153 (39%) underwent cEEG monitoring. Of those monitored, 86 EEGs (56%) met our inclusion criteria and were analyzed further (see Figure 1 for a detailed description of inclusions). The median age of the 86 included children at the time of CA was 2.6 years, and 62% were male. Main causes of CA were drowning and circulatory failure. Twelve months after CA, we observed a mortality rate of 56%; all children died before hospital discharge; the causes of death were predominantly withdrawal of life-sustaining therapies because of a poor neurologic prognosis (56%), followed by brain death (31%, Table 2).

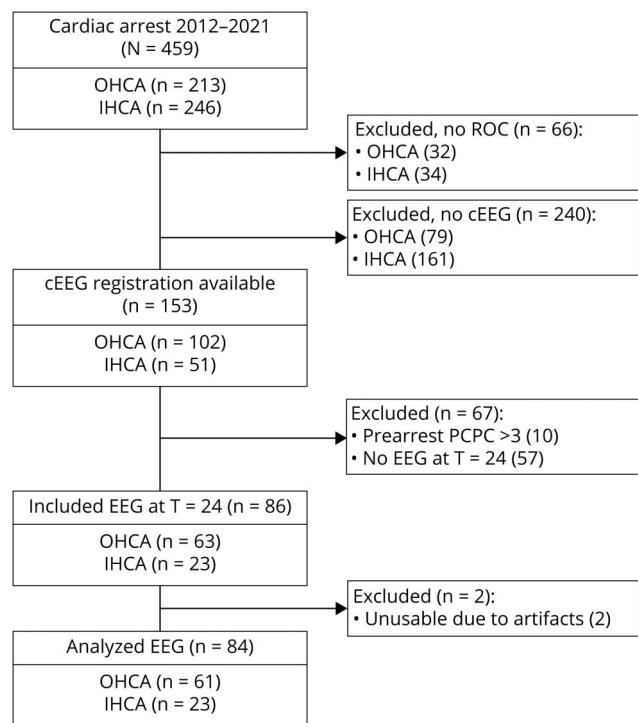
qEEG Results

The median time to initiate cEEG monitoring after CA was just over 10 hours (interquartile range 2.5–23.7 hours). Of

Table 2 Patient Cohort Characteristics

Age at CA, y, median (range)	2.6 (0.0–17.4)
Male sex, n (%)	53 (62)
Location of CA, n (%)	
Out of hospital	63 (73)
In hospital	23 (27)
Cause of arrest, n (%)	
Drowning	18 (21)
Circulatory failure	16 (19)
Respiratory failure	8 (9)
Airway obstruction	7 (8)
SIDS	7 (8)
Arrhythmia	7 (8)
Strangulation	6 (7)
Septic shock	4 (5)
Other	6 (7)
Cause unknown	7 (8)
Time between CA and start EEG, h, median (range)	10.5 (2.5–23.7)
Survival to hospital discharge, n (%)	38 (44)
PCPC after 12 mo, n (%)	
1	12 (14)
2	8 (9)
3	12 (14)
4	6 (7)
5	0 (0)
6	48 (56)
Cause of death (determined after 12 mo), n (%)	
WLST-neuro ^a	25 (52)
Brain death	15 (31)
Circulatory failure	4 (8)
Indirect causes ^b	3 (6)
Respiratory failure	1 (2)

Figure 1 Flowchart of Patient Inclusion and Exclusion Criteria



This diagram illustrates the patient population screened for inclusion in our study and reasons for exclusion. cEEG monitoring was more often used after OHCA compared with IHCA, likely because a larger proportion of the children with IHCA regained consciousness before monitoring could commence. cEEG = continuous EEG; IHCA = in-hospital cardiac arrest; OHCA = out-of-hospital cardiac arrest; ROC = return of circulation.

Abbreviations: CA = cardiac arrest; PCPC = Pediatric Cerebral Performance Category; SIDS = sudden infant death syndrome.

This table details the demographic and clinical profile of the 86 patients whose EEG data were included in the analysis. Data are presented as n (%) or median (range).

^a WLST-neuro denotes the withdrawal of life-sustaining therapies because of poor neurologic prognosis.

^b Indirect causes of death encompass events not directly stemming from the CA, for example, pulmonary hypertension due to preexisting pathology or complications of treatment such as intracranial hemorrhage during extracorporeal membrane oxygenation.

the 86 recordings available at T = 24, 2 were excluded because of excessive artifacts that hindered the accurate analysis of background patterns (Figure 1). A random forest model trained on EEG features obtained from the remaining 84 recordings at 24 hours after resuscitation was able to predict outcome after 12 months with an AUC of 0.90 (Figure 2). When integrating the prediction per epoch into an outcome per patient, the model obtained an accuracy of 0.77. All patients for whom the model predicted an unfavorable outcome indeed died within 12 months (positive predictive value and specificity = 1). However, the ability of the model to predict survival was lower because its prediction of a good outcome turned out to be false in 19 of 56 patients (negative predictive value of 0.66). The model did not predict an unfavorable outcome in all patients who died. This depended on the cause of death, with the model correctly predicting an unfavorable outcome in 27 of 39 deceased patients with a neurologic cause of death (a recall of 0.69). By contrast, it correctly predicted death only in 1 of 8 patients with a non-neurologic cause of death (recall of 0.13). For the population as a whole, the precision and recall for unfavorable outcomes are 1.0 and 0.60, respectively, resulting in an F1 score of 0.75.

To understand the contribution of specific EEG signal parameters on the model's predictions, we conducted a SHAP analysis. Among the features analyzed, the most

discriminating for predicting survival after 12 months are the minimal amplitude per EEG epoch and EEG silence ratio (ESR), a measure for signal continuity (Figure 3, A and B). Specifically, epochs with low minimal amplitude, indicative of low-voltage or even isoelectric EEG segments, strongly contribute to a prediction of poor outcome (shown in more detail in eFigure 2A). Similarly, a high ESR value, found in burst-suppression or isoelectric EEG backgrounds, significantly tilt the model toward predicting unfavorable outcome (eFigure 2B). Overall, EEG features related to amplitude and continuity contribute highly to the outcome of the model, whereas features encoding frequency, complexity, and connectivity have a lower impact (Figure 3, A and B). The distribution of SHAP values summarized in Figure 3C shows a nonuniform pattern, indicating distinct trajectories toward predicting either survival or death (illustrated in eFigure 3).

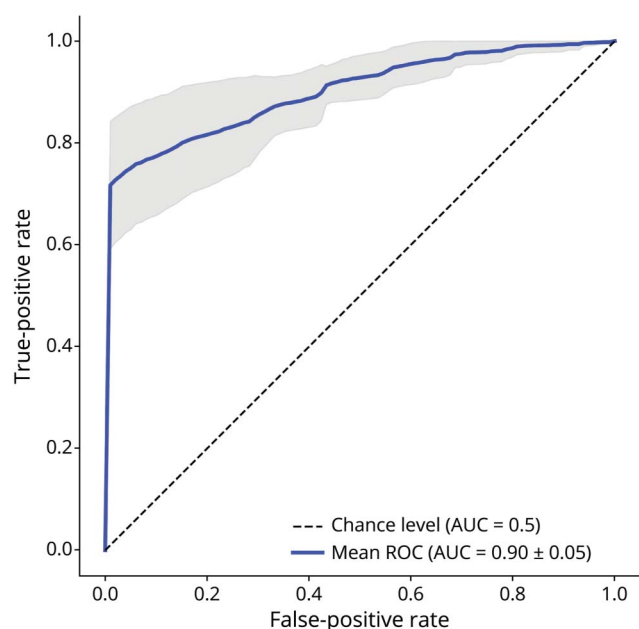
Visual EEG Results

To further investigate the relation between outcome and EEG background pattern, we also conducted a visual analysis of all EEG data used as training input for the random forest model. At 24 hours after CA, the EEG background pattern in most of the patients (59%) was classified as continuous with amplitudes above 20 μV (Table 3). Interobserver agreement on the classification of EEG background patterns was high, as indicated by a Cohen κ of 0.91. Interobserver disagreement focused on the distinction between identical and nonidentical bursts and differentiating between short bursts and GPDs.

There is a strong correlation between the EEG background pattern 24 hours after CA and outcome after 12 months. Specifically, of the 51 children with a continuous background pattern with amplitudes above 20 μV , 37 (73%) were still alive at 12 months. Conversely, in the group of 33 children with any of the alternative background patterns, not a single child survived (specificity = 1, Figure 4).

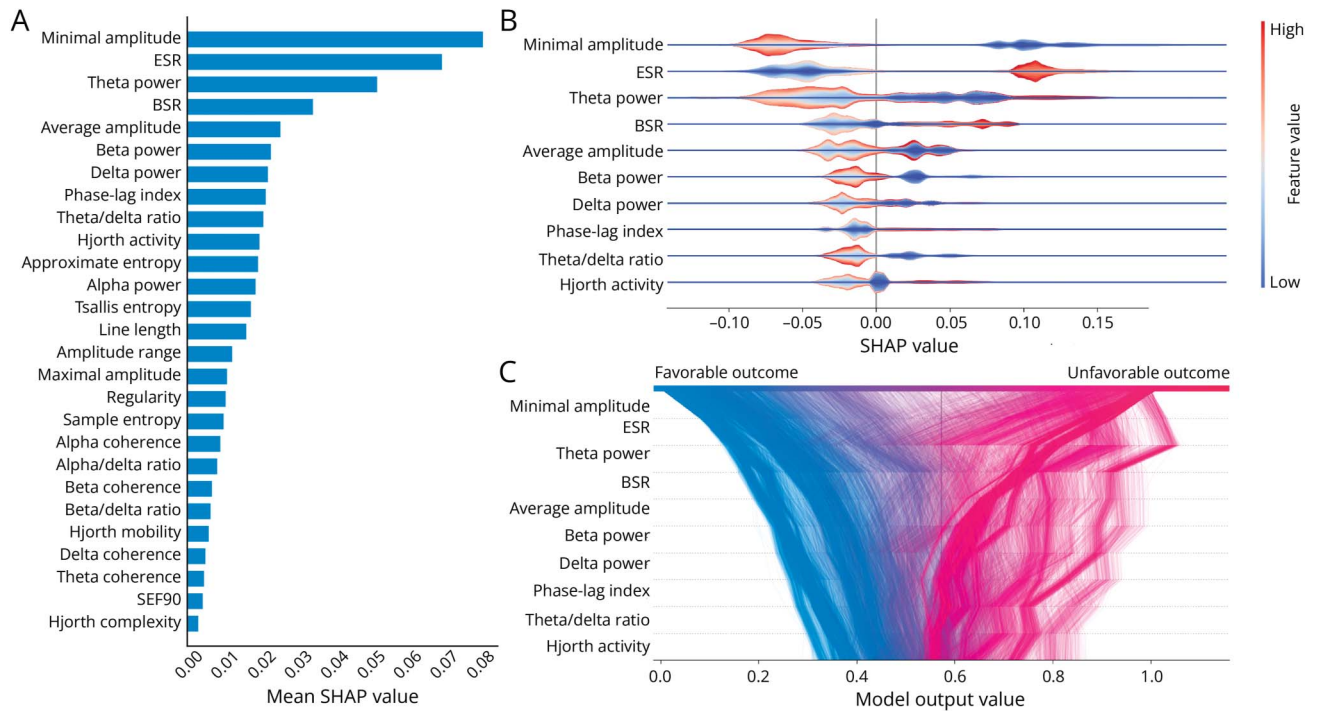
The agreement between EEG background patterns classified as other than continuous with amplitudes exceeding 20 μV , compared with the prediction of the random forest model is substantial, with a Cohen κ of 0.77, also reflected in a comparable accuracy of 0.83 (visual analysis) vs 0.77 (qEEG analysis). Disagreement mainly occurs in patients with either a continuous background or a burst-suppression pattern (see eFigure 4). In some patients with a continuous background pattern with normal amplitudes, a minority of epochs has either relatively low background amplitude or large fluctuations in amplitude, mimicking a low-voltage or burst-suppression pattern (illustrated in eFigure 5). On the other hand, some EEGs with a burst-suppression background pattern contain frequent or long bursts that last the whole duration of an epoch. In these cases, because of the high level of continuity and high amplitudes, the model does not predict an unfavorable outcome for these patients (examples shown in eFigure 6).

Figure 2 Random Forest Model Performance Using Quantitative EEG Features for 12-Month Mortality Prediction



The receiver-operating characteristic curve shows the true-positive rate as a function of the false-positive rate for the prediction of survival after 12 months for each EEG epoch, with an average AUC of 0.90 (\pm SD in gray) across 5 different training folds, suggesting robust predictive capability. AUC = area under the curve.

Figure 3 SHAP Value Analysis of the 10 Most Predictive Features in the Random Forest Model for 12-Month Survival Prediction



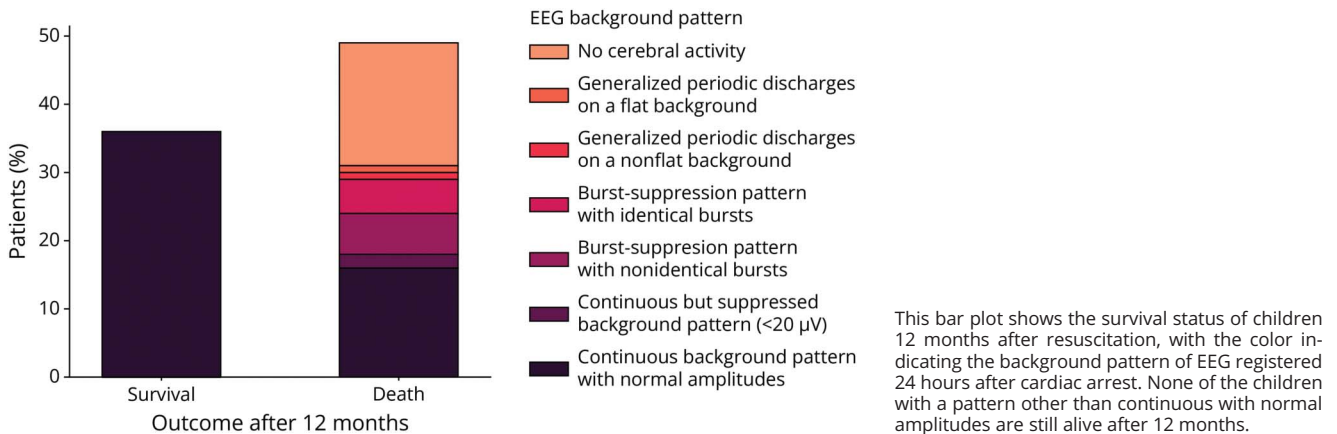
Panel A: For each of the EEG features included in the random forest model, the average absolute SHAP value is shown, with higher values indicating a stronger contribution to the classification. See Table 3 for explanation of the features. Panel B presents a summary plot, showing the impact of each feature on the model's predictions. The colors represent feature values, with red indicating high values and blue indicating low values. The horizontal axis shows the SHAP value, which reflects how much each feature influences the model's output, shifting the prediction from the baseline risk of an unfavorable outcome in the entire population. Features with a positive SHAP value increase the likelihood of a prediction of unfavorable outcome while a negative SHAP value reduces this likelihood. For example, a high minimal amplitude (first row, in red) reduces the likelihood of a prediction of unfavorable outcome while a low minimal amplitude (first row, in blue) strongly increases this likelihood. A similar though opposite pattern is seen for the ESR in the second row, where low values (blue, indicating a continuous EEG) are associated with a reduced likelihood of prediction of unfavorable outcome while high values (red, indicating a discontinuous EEG) increase this likelihood. Panel C: This decision plot maps the contributions of the top 10 features to the model's prediction per EEG epoch, with each line depicting the prediction path for a single epoch. Starting at the bottom from a baseline risk of approximately 0.6, the plot shows how each feature incrementally increases or decreases the predicted risk. Blue lines indicate trajectories for epochs with a predicted favorable outcome and red lines for an unfavorable outcome. All 3 panels are based on the classifications of individual EEG epochs. Through these plots, we can dissect the model's reasoning, making the predictive process more interpretable. Decision plots for subsets of epochs based on true outcome, visual EEG background category, and cause of death are shown in Figure S3. BSR = burst-suppression ratio; ESR = EEG silence ratio; SHAP = Shapley Additive Explanations.

Table 3 Results of Visual Analysis of EEG Background Patterns

EEG background pattern at T = 24 after CA, n (%)	Total (N = 86)	OHCA (N = 63)	IHCA (N = 23)
Unusable due to artifacts	2 (2)	2 (3)	0 (0)
Continuous background pattern with amplitudes $\geq 20 \mu\text{V}$	51 (59)	32 (51)	19 (82)
Continuous but suppressed background pattern ($< 20 \mu\text{V}$)	2 (2)	1 (2)	1 (4)
Burst-suppression pattern with nonidentical bursts	6 (7)	5 (8)	1 (4)
Burst-suppression pattern with identical bursts	5 (6)	5 (8)	0 (0)
GPDs on a nonflat background	1 (1)	1 (2)	0 (0)
GPDs on a flat background	1 (1)	1 (2)	0 (0)
No cerebral activity	18 (21)	16 (25)	2 (9)

Abbreviations: CA = cardiac arrest; GPD = generalized periodic discharge; IHCA = in-hospital cardiac arrest; OHCA = out-of-hospital cardiac arrest. This table presents an overview of the results of visual analysis of the EEG background patterns at 24 hours after CA, comparing patterns across the entire patient cohort and divided by location of arrest (IHCA vs OHCA).

Figure 4 Relationship Between EEG Background Pattern 24 Hours After Cardiac Arrest and Survival Status After 12 Months



Discussion

This retrospective study of EEG acquired 24 hours after CA in 84 unconscious children examined the relationship between background patterns and survival outcomes after 12 months. A random forest model trained on specific qEEG features was able to predict an unfavorable outcome with high specificity, based mainly on continuity and amplitude of the EEG signal. These findings were confirmed through visual analysis, using a classification according to the ACNS Critical Care EEG criteria. In both approaches, we found that a discontinuous and/or low-amplitude EEG background pattern at 24 hours after resuscitation was strongly associated with death by 12 months. Based on both the random forest classifier and the visual background classification, none of the surviving children were incorrectly predicted to have an unfavorable outcome. This is essential in clinical settings because erroneous predictions of unfavorable outcomes could lead to premature withdrawal of care in a patient who might otherwise have had a good outcome. The findings highlight the potential of combining the objective qEEG analysis, supported by a ML algorithm, with the clinically well-established visual analysis of EEG to enhance the precision of neurologic prognostication in pediatric CA.

The contrast in EEG backgrounds between survival and death observed in our study appears more distinct compared to previously published results.^{13,16} These studies reported that some patients can fully recover, despite an initially abnormal, even flat EEG background pattern. This discrepancy may stem from the timing of EEG. Studies on the prognostic value of EEG background patterns in adults, which benefit from larger cohorts, have shown that the significance of specific patterns changes during the first 48 hours after resuscitation. A notable example is a discontinuous background pattern

with normal amplitudes, which suggests a favorable prognosis when observed within the first 12 hours after CA, whereas the same pattern after 24 hours is associated with an unfavorable outcome.³⁴ In children, the background pattern has been reported to be more stable.³⁵ In line with the recommendations in the Dutch national adult guideline on prognostication in postanoxic coma, in this study, automated and visual analysis of the EEG was performed 24 hours after resuscitation, a timing that may capture these critical prognostic shifts.

Another critical factor influencing the differences with previously published studies is the more severely affected patient population in our study, with a larger fraction of patients with OHCA vs IHCA, increased prevalence of isoelectric EEG background patterns, and a higher mortality rate. Between 2012 and 2016, cEEG was not the standard of care in unconscious children after CA; this might have created a selection bias in the first 5 years of the study. It is highly probable that more severely affected children were the ones being monitored. These findings underscore the importance of considering patient demographics and EEG timing in interpreting the prognostic value of EEG patterns. Besides, the causes of CA were diverse, with drowning as the most common cause. The question arises as to whether our findings can be extrapolated to encompass all causes of CA.

A key strength of this study is that it blends the results of qEEG analysis as input to a ML model, specifically a random forest classifier, with the nuanced visual analysis performed by experienced clinical neurophysiologists. While more complex prediction models using deep learning algorithms may offer better predictive performance,³⁶ they often lack explainability—a critical aspect when decisions about continuation of treatment in a child after CA depend on the

interpretability of the predictive model. By contrast, the random forest model offers a distinct advantage in this regard because the contribution of each EEG feature to prediction of a specific outcome can be reconstructed for each individual EEG epoch, allowing identification of EEG background patterns with prognostic significance. The ability to explain and understand predictions made by the model is not just a technical advantage, but a clinical necessity, ensuring that treatment decisions are well-informed and tailored to the situation of the individual patient.

One notable challenge in the use of qEEG parameters as training input for the model lies in the initial selection of features, which is based on our prior expectations regarding their predictive capabilities. This approach overlooks EEG features which may not be readily observed by a human reviewer, but could still hold significant prognostic value. In addition, this method only analyzes 1 short EEG fragment at a time, ignoring processes that take place over longer time scales, such as alternations between long bursts and suppressions. Consequently, this could lead to a suboptimal utilization of all the information potentially contained within the EEG signal. To mitigate this risk, we used a broad set of features from different signal domains—including frequency, entropy, and connectivity measures—to ensure a more holistic approach. Refining the process of feature selection to capture an even broader spectrum of the EEG's informational content remains a pivotal point of attention for future research, as is including features from other modalities (such as MRI³⁷). The use of different modalities could also mitigate the inherent limitations of EEG in detecting prognostic indicators unrelated to neurologic function, improving prediction of prognosis in children with a non-neurologic cause of death.

A significant limitation of this study is the small sample size, similar to other published investigations of pediatric CA. The limited number of training samples available can lead to model overfitting—where the model becomes too tailored to the training data, diminishing its generalizability—and validation in an independent data set is an essential next step. Moreover, special caution should be taken when interpreting the prognostic value of background patterns, which are scarce in our population, such as low-voltage or GPDs. All EEG registrations were performed in sedated patients, with levels of sedative drugs similar across all patients. The effect of sedation, especially propofol, has been described in detail in adult post-CA patients.³⁸ Although the effects on visual background classification are limited, sedation with propofol can lead to slight reductions in EEG amplitude and continuity, and similar changes are seen with midazolam.^{39,40} This could make it more difficult to translate the findings of our ML model to centers where different sedation protocols are used. Moving forward, it is imperative to seek larger, independent data sets for validation to ensure the robustness of the findings in this study.

In this study, the primary goal was to assess outcome using a simple assessment tool (PCPC), a widely recognized tool

for evaluating pediatric neurologic outcome after CA, which we further simplified into binary categories (survival or death) for training the random forest model. It is desirable to train this model on a more detailed PCPC score, preferably classifying on individual PCPC outcome labels. Still, the PCPC is a crude score, and a more detailed assessment of long-term neurobehavioral outcome is needed to provide clinicians and caretakers with information to guide treatment and supportive care.⁴¹ Future research could use a methodology similar as described in this study to identify EEG signal features that correlate with specific levels of cognitive outcomes, offering a more nuanced understanding of patient prognosis and potentially aiding in the development and evaluation of targeted therapeutic strategies.

A key issue with studies investigating prognostic accuracy is the risk of a self-fulfilling prophecy, where prediction of outcome increases its probability.⁴²⁻⁴⁴ To address this issue, we meticulously designed our study to minimize bias. All analyses of EEG, both quantitative and visual, were conducted offline, and the results were not available to the clinical team during the period where decisions regarding withdrawal of care were taken. The clinical neurophysiologists performing the visual analysis were blinded to patient outcome. However, the attending neurologists and intensive care physicians had access to the raw EEG data during stay of the patient in the PICU. In all cases where a decision to withdraw life-sustaining therapies was taken based on expected poor neurologic prognosis, this decision was primarily based on the results of neurologic examination (absence of brain stem reflexes) and Glasgow Coma Scale M1 (no motor response), as described in detail in a previous study.⁶

In summary, our analysis showed that EEG background patterns with discontinuous or low-amplitude activity 24 hours after CA had a high specificity for mortality. This conclusion is supported by both a ML model and traditional visual classification methods. Given the predominance of patients with OHCA and a higher mortality rate in our study cohort compared with other published reports, care should be taken when extrapolating these findings to other populations. The distinct characteristics of our cohort underscore the need for tailored prognostic assessments in CA cases. Future research should explore the applicability of the EEG patterns across diverse patient demographics to enhance the precision of post-CA prognosis and inform clinical decisions and care strategies.

Study Funding

No targeted funding reported.

Disclosure

The authors report no relevant disclosures. Go to Neurology.org/N for full disclosures.

Publication History

Received by *Neurology* April 26, 2024. Accepted in final form September 17, 2024. Submitted and externally peer reviewed. The handling editor was Associate Editor Courtney Wusthoff, MD, MS.

Appendix Authors

Name	Location	Contribution
Maayke Hunfeld, MD, PhD	Department of Neonatal and Pediatric Intensive Care, Division of Pediatric Intensive Care, Erasmus MC Children's Hospital, Rotterdam, the Netherlands	Drafting/revision of the manuscript for content, including medical writing for content; major role in the acquisition of data; study concept or design
Marit Verboom, MSc	Department of Neurology, Erasmus MC, University Medical Center, Rotterdam, the Netherlands	Drafting/revision of the manuscript for content, including medical writing for content; analysis or interpretation of data
Sabine Josemans, MSc	Department of Neurology, Erasmus MC, University Medical Center, Rotterdam, the Netherlands	Drafting/revision of the manuscript for content, including medical writing for content; analysis or interpretation of data
Annemiek van Ravensberg, MSc	Department of Neurology, Erasmus MC, University Medical Center, Rotterdam, the Netherlands	Drafting/revision of the manuscript for content, including medical writing for content; analysis or interpretation of data
Dirk Straver, MD, PhD	Department of Neurology, Erasmus MC, University Medical Center, Rotterdam, the Netherlands	Drafting/revision of the manuscript for content, including medical writing for content; analysis or interpretation of data
Femke Lückcrath, MSc	Delft Institute of Applied Mathematics, Delft University of Technology, the Netherlands	Drafting/revision of the manuscript for content, including medical writing for content; analysis or interpretation of data
Geurt Jongbloed, PhD	Delft Institute of Applied Mathematics, Delft University of Technology, the Netherlands	Drafting/revision of the manuscript for content, including medical writing for content; analysis or interpretation of data
Corinne Buysse, MD, PhD	Department of Neonatal and Pediatric Intensive Care, Division of Pediatric Intensive Care, Erasmus MC Children's Hospital, Rotterdam, the Netherlands	Drafting/revision of the manuscript for content, including medical writing for content; study concept or design
Robert van den Berg, MD, PhD	Department of Neurology, Erasmus MC, University Medical Center, Rotterdam, the Netherlands	Drafting/revision of the manuscript for content, including medical writing for content; major role in the acquisition of data; study concept or design; analysis or interpretation of data

References

1. Holmberg MJ, Ross CE, Fitzmaurice GM, et al. Annual incidence of adult and pediatric in-hospital cardiac arrest in the United States. *Circ Cardiovasc Qual Outcomes*. 2019;12(7):e005580. doi:10.1161/circoutcomes.119.005580

2. Atkins DL, Everson-Stewart S, Sears GK, et al. Epidemiology and outcomes from out-of-hospital cardiac arrest in children: the Resuscitation Outcomes Consortium Epistry-Cardiac Arrest. *Circulation*. 2009;119(11):1484-1491. doi:10.1161/CIRCULATIONAHA.108.802678

3. Topjian AA, Berg RA. Pediatric out-of-hospital cardiac arrest. *Circulation*. 2012;125(19):2374-2378. doi:10.1161/CIRCULATIONAHA.111.071472

4. Girotra S, Spertus JA, Li Y, et al. Survival trends in pediatric in-hospital cardiac arrests: an analysis from get with the guidelines-resuscitation. *Circ Cardiovasc Qual Outcomes*. 2013;6(1):42-49. doi:10.1161/CIRCOUTCOMES.112.967968

5. Bimerew M, Wondmieni A, Gedefaw G, Gebremeskel T, Demis A, Getie A. Survival of pediatric patients after cardiopulmonary resuscitation for in-hospital cardiac arrest: a systematic review and meta-analysis. *J Pediatr*. 2021;47(1):118. doi:10.1186/s13052-021-01058-9

6. Hunfeld M, Nadkarni VM, Topjian A, et al. Timing and cause of death in children following return of circulation after out-of-hospital cardiac arrest: a single-center retrospective cohort study. *Pediatr Crit Care Med*. 2021;22(1):101-113. doi:10.1097/PCC.0000000000002577

7. Tsao CW, Aday AW, Almarzoq ZI, et al. Heart disease and stroke statistics—2023 update: a report from the American Heart Association. *Circulation*. 2023;147(8):e93-e621. doi:10.1161/CIR.0000000000001123

8. Hunfeld M, Ketharanathan N, Catsman C, et al. A systematic review of neuro-monitoring modalities in children beyond neonatal period after cardiac arrest. *Pediatr Crit Care Med*. 2020;21(10):E927-E933. doi:10.1097/PCC.0000000000002415

9. Slovis JC, Bach A, Beaulieu F, Zuckerberg G, Topjian A, Kirschen MP. Neuro-monitoring after pediatric cardiac arrest: cerebral physiology and injury stratification. *Neurocrit Care*. 2024;40(1):99-115. doi:10.1007/s12028-023-01685-6

10. Kirschen MP, Walter JK. Ethical issues in neuroprognostication after severe pediatric brain injury. *Semin Pediatr Neurol*. 2015;22(3):187-195. doi:10.1016/j.spen.2015.05.004

11. Sandroni C, D'Arrigo S, Cacciola S, et al. Prediction of poor neurological outcome in comatose survivors of cardiac arrest: a systematic review. *Intensive Care Med*. 2020;46(10):1803-1851. doi:10.1007/s00134-020-06198-w

12. Sandroni C, D'Arrigo S, Cacciola S, et al. Prediction of good neurological outcome in comatose survivors of cardiac arrest: a systematic review. *Intensive Care Med*. 2022;48(4):389-413. doi:10.1007/s00134-022-06618-z

13. Topjian AA, Sánchez SM, Shults J, Berg RA, Dlugos DJ, Abend NS. Early electroencephalographic background features predict outcomes in children resuscitated from cardiac arrest. *Pediatr Crit Care Med*. 2016;17(6):547-557. doi:10.1097/PCC.0000000000000740

14. Ostendorf AP, Hartman ME, Friess SH. Early electroencephalographic findings correlate with neurologic outcome in children following cardiac arrest. *Pediatr Crit Care Med*. 2016;17(7):667-676. doi:10.1097/PCC.0000000000000791

15. Ducharme-Crevier L, Press CA, Kurz JE, Mills MG, Goldstein JL, Wainwright MS. Early presence of sleep spindles on electroencephalography is associated with good outcome after pediatric cardiac arrest. *Pediatr Crit Care Med*. 2017;18(5):452-460. doi:10.1097/PCC.0000000000001137

16. Fung FW, Topjian AA, Xiao R, Abend NS. Early EEG features for outcome prediction after cardiac arrest in children. *J Clin Neurophysiol*. 2019;36(5):349-357. doi:10.1097/WNP.0000000000000591

17. Abend NS, Massey SL, Fitzgerald M, et al. Interrater agreement of EEG interpretation after pediatric cardiac arrest using standardized critical care EEG terminology. *J Clin Neurophysiol*. 2017;34(6):534-541. doi:10.1097/WNP.0000000000000424

18. Tjepkema-Cloostermans MC, van Meulen FB, Meinsma G, van Putten MJAM. A Cerebral Recovery Index (CRI) for early prognosis in patients after cardiac arrest. *Crit Care*. 2013;17(5):R252. doi:10.1186/cc13078

19. Keijzer HM, Tjepkema-Cloostermans MC, Klijn CJM, Blans M, van Putten MJAM, Hofmeijer J. Dynamic functional connectivity of the EEG in relation to outcome of post-anoxic coma. *Clin Neurophysiol*. 2021;132(1):157-164. doi:10.1016/j.clinph.2020.10.024

20. Amorim E, van der Stoep M, Nagaraj SB, et al. Quantitative EEG reactivity and machine learning for prognostication in hypoxic-ischemic brain injury. *Clin Neurophysiol*. 2019;130(10):1908-1916. doi:10.1016/j.clinph.2019.07.014

21. Lee S, Zhao X, Davis KA, Topjian AA, Litt B, Abend NS. Quantitative EEG predicts outcomes in children after cardiac arrest. *Neurology*. 2019;92(20):E2329-E2338. doi:10.1212/WNL.0000000000007504

22. Sanssevere AJ, Janatti A, DiBacco ML, Cavan K, Rotenberg A. Background EEG suppression ratio for early detection of cerebral injury in pediatric cardiac arrest. *Neurocrit Care*. 2024;41(1):156-164. doi:10.1007/s12028-023-01920-0

23. Fiser DH. Assessing the outcome of pediatric intensive care. *J Pediatr*. 1992;121(1):68-74. doi:10.1016/s0022-3476(05)82544-2

24. Kemp B, Oliván J. European data format 'plus' (EDF+), an EDF alike standard format for the exchange of physiological data. *Clin Neurophysiol*. 2003;114(9):1755-1761. doi:10.1016/s1388-2457(03)00123-8

25. Pernet CR, Appelhoff S, Gorgolewski KJ, et al. EEG-BIDS, an extension to the brain imaging data structure for electroencephalography. *Sci Data*. 2019;6(1):103. doi:10.1038/s41597-019-0104-8

26. Sondag L, Ruijter BJ, Tjepkema-Cloostermans MC, et al. Early EEG for outcome prediction of postanoxic coma: prospective cohort study with cost-minimization analysis. *Crit Care*. 2017;21(1):111. doi:10.1186/s13054-017-1693-2

27. Gramfort A, Luessi M, Larson E, et al. MEG and EEG data analysis with MNE-Python. *Front Neurosci*. 2013;7:267. doi:10.3389/fnins.2013.00267

28. Ghassemi MM, Amorim E, Alhanai T, et al. Quantitative electroencephalogram trends predict recovery in hypoxic-ischemic encephalopathy. *Crit Care Med*. 2019;47(10):1416-1423. doi:10.1097/CCM.0000000000003840

29. Noirhomme Q, Lehembre R, Lugo ZDR, et al. Automated analysis of background EEG and reactivity during therapeutic hypothermia in comatose patients after cardiac arrest. *Clin EEG Neurosci*. 2014;45(1):6-13. doi:10.1177/1550059413509616
30. MATLAB. The MathWorks Inc.; 2022.
31. Pedregosa F, Varoquaux G, Gramfort A, et al. Scikit-learn: machine learning in Python. *J Mach Learn Res*. 2011;12(85):2825-2830.
32. Lundberg SM, Erion G, Chen H, et al. From local explanations to global understanding with explainable AI for trees. *Nat Mach Intell*. 2020;2(1):56-67. doi:10.1038/s42256-019-0138-9
33. Hirsch LJ, Fong MWK, Leitinger M, et al. American Clinical Neurophysiology Society's standardized critical care EEG terminology: 2021 version. *J Clin Neurophysiol*. 2021;38:1-29. doi:10.1097/WNP.0000000000000806
34. Ruijter BJ, Tjepkema-Cloostermans MC, Tromp SC, et al. Early electroencephalography for outcome prediction of postanoxic coma: a prospective cohort study. *Ann Neurol*. 2019;86(2):203-214. doi:10.1002/ana.25518
35. Abend NS, Xiao R, Kessler SK, Topjian AA. Stability of early EEG background patterns after pediatric cardiac arrest. *J Clin Neurophysiol*. 2018;35(3):246-250. doi:10.1097/WNP.0000000000000458
36. Pham SDT, Keijzer HM, Ruijter BJ, et al. Outcome prediction of postanoxic coma: a comparison of automated electroencephalography analysis methods. *Neurocrit Care*. 2022;37(suppl 2):248-258. doi:10.1007/s12028-022-01449-8
37. Bach AM, Kirschen MP, Fung FW, et al. Association of EEG background with diffusion-weighted magnetic resonance neuroimaging and short-term outcomes after pediatric cardiac arrest. *Neurology*. 2024;102(5):e209134. doi:10.1212/WNL.000000000000209134
38. Ruijter BJ, van Putten MJAM, van den Bergh WM, Tromp SC, Hofmeijer J. Propofol does not affect the reliability of early EEG for outcome prediction of comatose patients after cardiac arrest. *Clin Neurophysiol*. 2019;130(8):1263-1270. doi:10.1016/j.clinph.2019.04.707
39. Veselis RA, Reinsel R, Marino P, Sommer S, Carlon GC. The effects of midazolam on the EEG during sedation of critically ill patients. *Anaesthesia*. 1993;48(6):463-470. doi:10.1111/j.1365-2044.1993.tb07063.x
40. Ter Horst HJ, Brouwer OF, Bos AF. Burst suppression on amplitude-integrated electroencephalogram may be induced by midazolam: a report on three cases. *Acta Paediatr*. 2004;93(4):559-563. doi:10.1080/08035250410022882
41. van Zelle L, Busse C, Madderom M, et al. Long-term neuropsychological outcomes in children and adolescents after cardiac arrest. *Intensive Care Med*. 2015;41(6):1057-1066. doi:10.1007/s00134-015-3789-y
42. Hofmeijer J, Beernink TMJ, Bosch FH, Beishuizen A, Tjepkema-Cloostermans MC, van Putten MJAM. Early EEG contributes to multimodal outcome prediction of postanoxic coma. *Neurology*. 2015;85(2):137-143. doi:10.1212/WNL.0000000000001742
43. Rossetti AO, Rabinstein AA, Oddo M. Neurological prognostication of outcome in patients in coma after cardiac arrest. *Lancet Neurol*. 2016;15(6):597-609. doi:10.1016/S1474-4422(16)00015-6
44. Oddo M, Rossetti AO. Early multimodal outcome prediction after cardiac arrest in patients treated with hypothermia. *Crit Care Med*. 2014;42(6):1340-1347. doi:10.1097/CCM.0000000000000211
45. Koolen N, Jansen K, Vervisch J, et al. Line length as a robust method to detect high-activity events: automated burst detection in premature EEG recordings. *Clin Neurophysiol*. 2014;125(10):1985-1994. doi:10.1016/j.clinph.2014.02.015
46. Martínez-Cagigal V. *Sample Entropy*. MathWorks; 2018.
47. Tsallis C. Possible generalization of Boltzmann-Gibbs statistics. *J Stat Phys*. 1988;52(1-2):479-487. doi:10.1007/bf01016429
48. Stam CJ, Nolte G, Daffertshofer A. Phase lag index: assessment of functional connectivity from multi channel EEG and MEG with diminished bias from common sources. *Hum Brain Mapp*. 2007;28(11):1178-1193. doi:10.1002/hbm.20346
49. Theilen HJ, Ragaller M, Tschö U, May SA, Schackert G, Albrecht MD. Electroencephalogram silence ratio for early outcome prognosis in severe head trauma. *Crit Care Med*. 2000;28(10):3522-3529. doi:10.1097/00003246-200010000-00029
50. Hjorth BO. EEG analysis based on time domain properties. *Electroencephalogr Clin Neurophysiol*. 1970;29(3):306-310. doi:10.1016/0013-4694(70)90143-4